Late Onset Death of Motor Neurons in Mice Overexpressing Wild-Type Peripherin

Jean-Martin Beaulieu, Minh Dang Nguyen, and Jean-Pierre Julien

Centre for Research in Neurosciences, McGill University, The Montréal General Hospital Research Institute, Montréal, Québec, H3G 1A4, Canada

Abstract. Peripherin, a type III intermediate filament (IF) protein, upregulated by injury and inflammatory cytokines, is a component of IF inclusion bodies associated with degenerating motor neurons in sporadic amyotrophic lateral sclerosis (ALS). We report here that sustained overexpression of wild-type peripherin in mice provokes massive and selective degeneration of motor axons during aging. Remarkably, the onset of peripherin-mediated disease was precipitated by a deficiency of neurofilament light (NF-L) protein, a phenomenon associated with sporadic ALS. In NF-L null mice, the overexpression of peripherin led to early-onset formation of IF inclusions and to the selective death of spinal motor neurons at 6 mo of age. We also report the formation of similar peripherin inclusions in presymptomatic transgenic mice expressing a mutant form of superoxide dismutase linked to ALS. Taken together, these results suggest that IF inclusions containing peripherin may play a contributory role in motor neuron disease.

Key words: peripherin • neurofilament • ALS • motor neuron • transgenic

AMYOTROPHIC lateral sclerosis (ALS)[1] is an adult-onset neurological disorder that affects primarily motor neurons in the brain and spinal cord. The degeneration of motor neurons leads to atrophy of skeletal muscles and, ultimately, to paralysis and death. Approximately 10% of the ALS cases are familial with the disease inherited in an autosomal dominant manner. Mutations in the copper/zinc superoxide dismutase (SOD1) gene have been found in ~20% of familial cases (2% of total ALS cases) (Rosen et al., 1993). Whereas transgenic mouse studies provided compelling evidence that SOD1 mutations cause ALS through a gain of deleterious activities (Gurney et al., 1994; Wong et al., 1995; Ripps et al., 1995; Tu et al., 1996; Bruijn et al., 1997, 1998), the etiology of ALS remains unknown for the vast majority of sporadic and familial cases. One hallmark of ALS is the presence of cytoplasmic inclusions of disorganized proteins in the cytoplasm of motor neurons (reviewed in Chou, 1995). Some inclusions have been shown to contain mutant SOD1 protein (Kato et al., 1996; Shibata et al., 1996; Bruijn et al., 1998), whereas others contain neuronal intermediate filament (IF) proteins (Carpenter, 1968; Tu et al., 1996).

Peripherin is a type III neuronal IF protein of 57 kD which is found with neurofilament (NF) proteins in the majority of IF inclusions (89%) in motor neurons of ALS patients (Corbo and Hays, 1992; Migheli et al., 1993; Tu et al., 1996). In adults, peripherin is mostly expressed in autonomic nerves and in peripheral sensory neurons with only low levels detectable in spinal motor neurons (Parysek and Goldman, 1988; Brody et al., 1989; Escurat et al., 1990; Troy et al., 1990a,b). However, peripherin gene expression is increased by up to 300% in spinal motor neurons after injury of the sciatic nerve (Troy et al., 1990a), whereas expression of all three NF subunits mRNAs is reduced (Muma et al., 1990). Inflammation is one mechanism that can explain the upregulation of peripherin in injured neurons. In fact, peripherin gene expression is upregulated by the inflammatory cytokines interleukin-6 (IL-6) and leukemia inhibitory factor (LIF; Djabali et al., 1993; Sterneck et al., 1996) through the action of a JAK/STAT signaling pathway activating the STAT 1 and STAT 3 transcription factors (Lecomte et al., 1998). The action of cytokines on peripherin expression suggests that an upregulation of peripherin may be part of a general response of motor neurons to noxious stress that may explain the presence of nu-

Address correspondence to Dr. Jean-Pierre Julien, The Montréal General Hospital Research Institute, 1650 Cedar Avenue, Montréal, Québec, H3G 1A4, Canada. Tel.: (514) 934-8058. Fax: (514) 934-8265. E-mail: mdju@musica.mcgill.ca

1. *Abbreviations used in this paper:* ALS, amyotrophic lateral sclerosis; DRG, dorsal root ganglion; IF, intermediate filament; IL-6, interleukin 6; LIF, leukemia inhibitory factor; NF, neurofilament; NF-H, neurofilament heavy subunit; NF-L, neurofilament light subunit; NF-M, neurofilament medium subunit; SOD1, copper/zinc superoxide dismutase; WT, wild-type.

merous peripherin inclusion bodies in motor neurons of ALS patients.

In contrast to NFs, which are obligate heteropolymers of three subunits (Ching and Liem, 1993; Lee et al., 1993), peripherin can self-assemble to establish an IF network in cultured cells (Cui et al., 1995; Ho et al., 1995; Beaulieu et al., 1999). Peripherin can also interact in vivo with NF proteins (Parysek et al., 1991) and can form heterodimers with each one of the three NF subunits in vitro (Athlan and Mushynski, 1997). We have recently studied the interactions of peripherin with NF proteins in cultured SW13 cells devoid of endogenous cytoplasmic IF proteins (Beaulieu et al., 1999). Our results showed that peripherin can assemble with NFs as well as with the light NF subunit (NF-L) protein alone to form an IF network. Unexpectedly, the expression of peripherin with the heavy NF subunits (NF-H or NF-M) in the absence of NF-L prevented the formation of an IF network in transfected cells (Beaulieu et al., 1999).

We have used a transgenic mouse approach to investigate the potential detrimental effects of a sustained peripherin overexpression in motor neurons. Our results show that an upregulation of peripherin in mice causes a late-onset and selective motor neuron disease characterized by the formation of IF inclusions similar to those found in human ALS and in mice expressing mutant form of SOD1 linked to ALS. Moreover, the formation of IF inclusion bodies and the onset of disease were precipitated by a deficiency in NF-L protein probably through a deleterious action of the large NF subunits on peripherin organization.

Materials and Methods

Transgenic and Knockout Mice

The DNA constructs used to produce mice expressing the mouse peripherin gene under the control of the human Thy-1 gene promoter were derived as followed. The Thy-1 regulatory sequences were isolated by long range PCR amplification (XL PCR™ system; Perkin Elmer) from a vector (pBSV; a gift of Dr. Vincent Giguère, McGill University, Montreal) containing the complete human Thy-1 gene (GenBank/EMBL/DDBJ accession number M11749) (van Rijs et al., 1985). The 5′ primer (TGCCCGCCTGATGAATGCTCATCCGGAATTC) corresponded to the vector sequence upstream from the Thy-1 locus in pBSV. The 3′ primer (GGATCCAGGACTGAGATCCCAGAACC) was complementary to the last 26 bp from the noncoding fraction of the second exon of the human Thy-1 gene. Both primers were purchased from GIBCO-BRL. The resulting 3.5-kb PCR product was digested with EcoRI to remove the pBSV sequence of the 5′ primer before its insertion in pBluescript SK+ (Stratagene) in the EcoRI to EcoRV orientation. The resulting vector included the promoter, the first exon, the first intron, and the complete 5′ noncoding region of the second exon of the human Thy-1 gene subcloned upstream of an HindIII site in the multicloning cassette of pBluescript SK+. A 5.9-kb peripherin fragment was then obtained by the Eco47III, EcoRV digestion of a bacteriophage clone containing the complete mouse peripherin locus (a gift from Dr. André Royal, Université de Montréal, Montréal). This fragment was subcloned into the HindIII site of the Thy-1 vector. The correct orientation of the peripherin fragment was confirmed by XhoI and ApaI digestion. The resulting construct (TPer) included the human Thy-1 gene regulatory sequences followed by the complete coding sequence of the mouse peripherin gene starting at 23 bp upstream of the putative translation start site (Cui et al., 1995; Ho et al., 1995) and ending 2.5 kb downstream of the polyadenylation signal (see Fig. 1 A).

The 9.5-kb DNA fragment (Per), used to derive mice expressing the mouse peripherin gene under the control of its own promoter element, was obtained by digestion of the original bacteriophage DNA with EcoRV. The Per fragment contained the complete peripherin gene along with 3.1 kb from the 5′ and 2.5 kb from the 3′ flanking genomic sequences (see Fig. 1 A).

The constructs were isolated from their vector sequences by digestion with endonuclease restriction enzymes followed by purification on agarose gels using a Gene Clean II Kit™ (Bio101). The resulting linear DNA fragments were microinjected into one-cell mouse embryos of C57Bl/C3H genetic background according to standard procedures (Brinster et al., 1981). The integration of the transgenes into mouse genomic DNA was confirmed by Southern blot analysis as described below.

Mice carrying the transgenes in NF-L null background were obtained by breeding transgenic mice with NF-L knockout mice (L−/− mice) (Zhu et al., 1997). The breeding was performed following a two-step procedure. In the first step, F1 transgenic mice were bred with NF-L knockout mice to generate mice carrying the transgene in an L+/− background. These mice were then backcrossed with L−/− mice leading to the production of mice carrying the transgene in L−/− background. All peripherin transgenic mice used in this study were heterozygous for the peripherin transgenes.

The $SOD1^{G37R}$ mice (Wong et al., 1995) were a kind gift of Drs. Donald L. Price (Johns Hopkins Medical School, Baltimore, MD) and Don Cleveland (Ludwig Institute, San Diego, CA).

Southern Blot Analysis

Southern blot analysis of genomic DNA isolated from mouse tails was carried out following procedures described previously (Côté et al., 1993). A 1.8-kb peripherin probe was generated by digestion of the Per DNA construct with EcoRI (see Fig. 1 A). This probe was designed for detection of a 1.8-kb band corresponding to the endogenous peripherin gene while the TPer transgene was detected as a 4.9-kb band. The probe and enzymatic digestion protocols used to detect the NF-L knockout genotype have been described previously (Zhu et al., 1997). The number of transgene copies inserted in the genome was estimated by Southern blotting with serial dilution of DNA extracted from F1 transgenic and nontransgenic mice from each line. The relative intensity of the bands was compared with the signal detected for the endogenous peripherin gene using Gel-pro 2.0.1 (Media Cybernetic) with a Power Macintosh computer.

Northern Blot Analysis

6-mo-old animals were killed by injection of an overdose of chloral hydrate. Tissues were collected, frozen in liquid nitrogen, and kept at −80°C before extraction of total RNA using the Trizol reagent™ (GIBCO-BRL). Total RNA (10 μg except 5 μg for dorsal root ganglia) were fractionated on 1% (wt/vol) agarose-formaldehyde gels, transferred to Gene screen plus™ membranes (NEN Life Science), hybridized, and washed according to standard procedures (Sambrook et al., 1989). The mRNA species were detected by autoradiography using Biomax MR™ film (Kodak) in the presence of an intensifying screen.

The actin probe corresponded to the complete cDNA from the rat β-actin. The peripherin probe corresponded to the first 538 bp of the peripherin transcript (GenBank/EMBL/DDBJ accession number X59840). This probe was derived by PCR from mouse genomic DNA using the (ATGAGCCATCATCACTCGTCGGGCC) 5′ primer and the (TCTGCTTGAGCGCCGCTAGGTCCT) 3′ primer. The NF-L probe was derived by PCR of the mouse NF-L first exon (GenBank/EMBL/DDBJ accession number M20480) using the (ATGAGTTCGTTCGGCTCGGATCCGAT) 5′ primer and the (CCTCATAGCGAGCCTGCAGGTTGCG) 3′ primer. The primers used to derive these two probes were purchased from GIBCO-BRL and the PCR reactions were carried out using Taq polymerase (Pharmacia). All probes were purified on agarose gels and labeled using the random primer method before hybridization (Feinberg and Vogelstein, 1983).

Antibodies

The anti-peripherin monoclonal antibody (MAB1527), the anti-peripherin polyclonal antibody (AB1530), and the anti α-internexin polyclonal antibody (AB1515) were from Chemicon. The anti-peripherin monoclonal antibody (NCL-Periph) was from Novocastra Laboratories Ltd. The anti–NF-H polyclonal antibody (N-4142) is from Sigma. The anti–NF-M monoclonal antibody (NN-18), the anti–NF-L monoclonal antibody (NR-4), the anti-hyperphosphorylated NF-H monoclonal antibody (RT-97), and the anti-actin clone c4 monoclonal antibody were from Boehringer Mannheim. The anti-hypophosphorylated NF-H monoclonal antibody (Smi-32) was from Steinberger Monoclonal Inc.

SDS-PAGE and Western Blot Analysis

6–10-mo-old mice (except if otherwise mentioned in figure legend) were killed and the tissues collected as for Northern blot analysis. For total protein extraction, tissues were homogenized in 0.5% (wt/vol) SDS, and 8 M urea (SDS/urea buffer). Preparation of the cytoskeletal insoluble proteins was carried out using a modified version of the method described by Ching and Liem (1993). Tissues were first homogenized at 48°C in a buffer containing Tris (10 mM), NaCl (150 mM), EDTA (1 mM), Triton X-100 (1% wt/vol), PMSF (2 mM), leupeptin (2 mg/ml), pepstatin (1 mg/ml), and aprotinin (10 mg/ml). The homogenates were then centrifuged at 14,000 *g* for 15 min at 4°C using a Sorvall MC-12V centrifugator (Dupont). The supernatants (soluble fraction) were collected and kept for further use. The pellets (insoluble fraction) were resuspended in a volume of SDS/urea buffer equivalent to the volume of the soluble fraction. The protein concentration in the different extracts was measured using the DC-Protein assay™, (BioRad). The protein extracts were diluted in 2× sample buffer (30% [wt/vol] glycerol, 4% [wt/vol] SDS, 160 mM Tris HCl [pH 6.8], 10% [vol/vol] β-mercaptoethanol and 0.02% [wt/vol] bromophenol blue) and boiled for 3 min. Proteins were separated on 8% or 10% SDS-PAGE and either transferred to a nitrocellulose membrane or stained with 0.2% (wt/vol) Coomassie blue-R250 in a 10% (vol/vol) acetic acid and 45% (vol/vol) methanol solution. Nitrocellulose membranes were blocked in PBS containing 5% (wt/vol) skimmed milk powder (PBS/milk) before incubation with the primary antibodies diluted as follows: MAB1527, NR-4, and NN-18, 1:1,000 dilution; AB1515 and N-4142, 1:2,000; anti-actin, 1:5,000. After incubation, the blots were rinsed in PBS containing 0.1% (wt/vol) of Tween-20 (PBS/Tween) and incubated for 1 h with the appropriate secondary antibody (anti–mouse IgG peroxidase or anti–rabbit IgG peroxidase from the Jackson ImmunoResearch Laboratories) diluted 1:1,000 in PBS/milk. The immune complexes were revealed using the RenaissanceÙ chemiluminescence reagents (NEN Life Science).

Immunohistological Analysis

Immunohistochemical analysis was carried out as described by Jacomy and Bosler (1995). Mice were anesthetized by injection of chloral hydrate and perfused with a 16-g/liter sodium cacodylate buffer (pH 7.5) followed by fixative (3% [vol/vol] glutaraldehyde in sodium cacodylate buffer). 50-μm tissue sections were prepared using a vibratome. Floating sections were rinsed in PBS and treated for 30 min with a 1% (wt/vol) sodium borohydride solution to reduce epitope masking by glutaraldehyde. Sections were then blocked for 1 h in a PBS solution containing 3% (wt/vol) BSA, 0.5% (vol/vol) Triton X-100, and 0.03% (wt/vol) hydrogen peroxide. Incubation with the various antibodies was performed overnight at room temperature with agitation in a PBS solution containing 3% (wt/vol) BSA and 0.05% (vol/vol) Triton X-100. The antibody labeling was developed using a Vector ABC kit (Vector Laboratories Ltd.) and Sigmafast™ tablets (Sigma).

For indirect double immunofluorescence analysis, mice were perfused with PBS (pH 7.5) followed by fixative (4% vol/vol paraformaldehyde in a phosphate buffered solution). Tissues were postfixed for 2 h in paraformaldehyde, rinsed in PBS, and incubated overnight in a 20% (wt/vol) phosphate-buffered sucrose solution. 20-μm tissue sections were prepared using a cryostat. Sections were then blocked for 30 min in a PBS solution containing 3% (wt/vol) BSA and 0.5% (vol/vol) Triton X-100. Incubation with mixtures of primary antibodies was performed overnight at room temperature in a PBS solution containing 3% (wt/vol) BSA and 0.05% (wt/vol) Triton X-100. Incubation with a mixture of the anti–mouse-FITC and anti–rabbit rhodamine-conjugated antibody (Jackson ImmunoResearch Laboratory) was carried out for one hour under the same conditions. The samples were finally mounted in Prolong™ (Molecular Probe, Inc.) and examined with a fluorescence microscope.

Morphology and Electron Microscopy

Tissue sections were prepared for embedding in Epon as described in Zhu et al. (1997). Thin sections were stained with Toluidine blue and examined under a light microscope. The counting of axons in the L5 ventral root was performed manually from photographs. For electron microscopy, ultrathin sections were stained with a lead citrate solution and examined with a Philips CM10 transmission electron microscope.

To evaluate the survival of spinal motor neurons, a portion of the spinal cord spanning 1-mm rostral to 1-mm caudal of the L5 ventral root entry point was dissected out from two 14-mo-old mice of each genotype. The spinal cord was then cut in 50-μm sections using a vibratome and stained with cresyl violet according to standard procedures (Bancroft and Stevens, 1990). The large motor neurons in the ventral horn were then counted with the help of a technician who ignored the genotypes of the mice. Since this method did not produce an equal number of sections from each sample, the mean number of motor neurons per ventral horn section was calculated and compared for each genotype.

Motor Dysfunction

To evaluate motor dysfunction in the mice, we simply measured their capacity to grasp a vertical grid. The mice were placed at the center of a horizontal grid. The grid was then moved slowly to a vertical position. The time spent by the mice on the vertical grid was measured for a maximum of 2 min. This test was performed using five mice of each genotype and was repeated three times on separate days for a total of 15 tests per genotype.

Results

Generation of Transgenic Mice Overexpressing the Wild-Type Mouse Peripherin Gene

Two different DNA constructs were microinjected to generate transgenic mice overexpressing the wild-type mouse peripherin gene in motor neurons. The first DNA construct, called TPer, included the promoter of the Thy-1 gene with noncoding sequences of exon 1 and 2 (van Rijs et al., 1985) fused to the mouse peripherin gene starting at 23 nucleotides upstream from the initiation codon (Fig. 1 A). The second DNA construct, called Per, consisted of the complete mouse peripherin gene with 3.4 kb of 5′ and 2.5 kb of 3′ untranslated sequences (Fig. 1 A).

Six founders were obtained for each DNA construct. After Northern blot analysis of nervous tissues, we focused our efforts on the characterization of two lines of transgenic mice, the TPer line carrying 4 integrated copies of the TPer construct, and the Per line bearing 20 copies of the Per construct (Fig. 1 B).

Northern blot analysis was carried out to study the expression pattern of peripherin mRNA in normal and transgenic mice. Peripherin mRNA was detected in dorsal root ganglia (DRG) of normal (WT) mice, TPer transgenic mice, and Per transgenic mice (Fig. 1 C). Peripherin mRNA was also detected in the brain but not in the cerebellum of the TPer mice (Fig. 1 C). No peripherin mRNA was detected in nonnervous tissues of transgenic mice (Fig. 1 C). A combination of immunohistochemistry and Western blot analysis using anti-peripherin monoclonal antibodies was carried out to further analyze the peripherin expression patterns in the transgenic lines. Our analysis of normal mice allowed the detection of peripherin in DRG, spinal cord, and some sensory fibers of the brain stem. The TPer line showed a larger expression pattern with the detection of peripherin in the brain, in the optic nerve, in some reticular neurons of the brainstem, in the mesencephalic trigeminal nucleus, in the motor nucleus of the trigeminal and facial nerves, in the nucleus ambiguous, in the ventral and dorsal columns of the spinal cord, in spinal motor neurons, and in DRG. The Per mice overexpressed peripherin in sensory and motor neurons from the spinal cord and brain stem but they did not express detectable levels of peripherin in the brain.

Densitometry of Western blots, made up by the serial dilution of total protein extracts from dorsal and ventral roots (Fig. 1 D), showed that as compared with WT mice

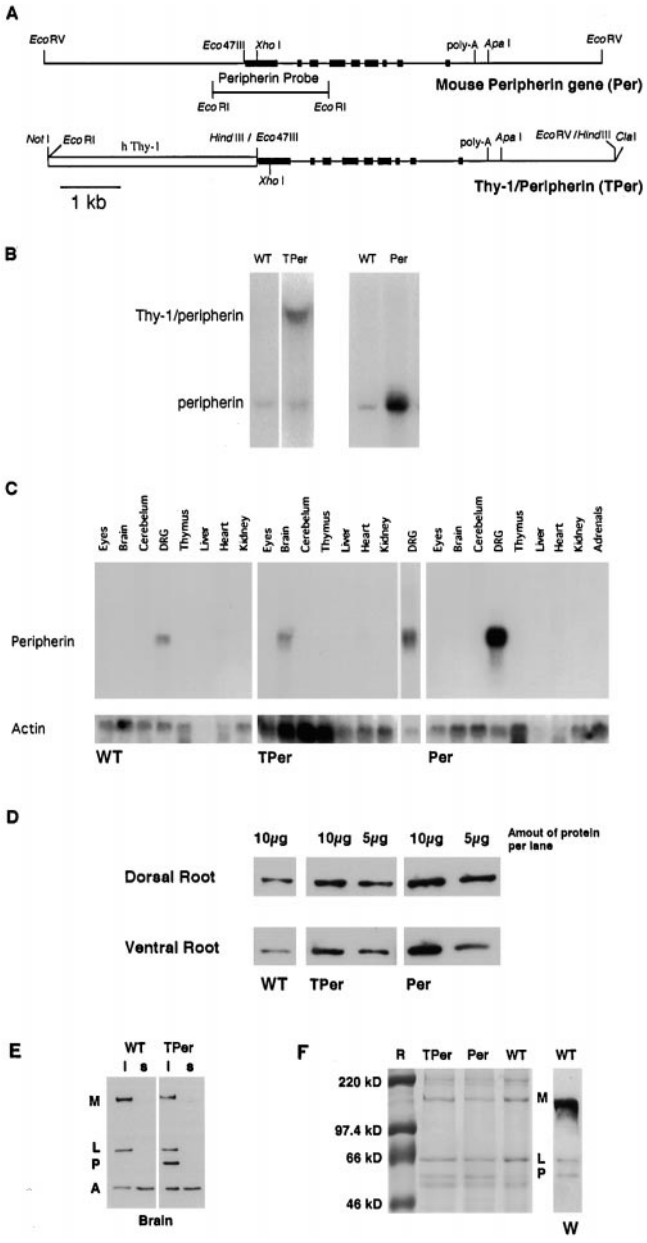

Figure 1. Transgenic mice overexpressing WT peripherin. (A) Partial restriction map of the Per and TPer DNA constructs. An Eco47III × EcoRV fragment of the mouse peripherin gene was subcloned downstream of the human Thy-1 gene promoter. Black boxes represent exons. The white box represents the 5′ transcriptional regulatory elements of the Thy-1 gene. The poly-A designates the polyadenylation signal of the peripherin gene. The peripherin probe used for the Southern blot analysis is indicated. (B) Southern blot analysis of genomic DNA extracted from the tails of control mice (WT) and of mice bearing the Per or TPer transgenes. (C) Northern blot showing expression of peripherin mRNA in different tissues of WT, TPer, and Per mice. (D) Western blot analysis of total protein extracts showing the increased peripherin levels in ventral and dorsal roots of TPer and Per transgenic mice. (E) Western blot analysis of soluble and insoluble protein extracts from the brain of WT and transgenic TPer mice. Two micrograms of insoluble protein extracts and an equivalent volume of soluble protein extracts were fractionated on SDS-PAGE and the blot was incubated with a mixture of monoclonal antibodies directed against NF-M (M), NF-L (L), peripherin (P), and actin (A). (F) Coomassie blue–stained SDS-PAGE of Triton X-100 insoluble fractions (20 μg) from the ventral roots showing the ratio of the peripherin (57-kD band) to NF-L (66-kD band) in WT and transgenic mouse extracts. R corresponds to a track loaded with the Rainbow molecular mass marker (GIBCO). The identity of the bands was confirmed by incubating a Western blot (W) of another part of the same gel with a mixture of antibodies against NF-M (M), NF-L (L), and peripherin (P).

Table I. Relative Protein Levels of Peripherin Compared with NF-L in Cytoskeletal Fractions of Dorsal and Ventral Roots

Tissues	Genotype	Ratio of peripherin to NF-L
Ventral root	WT ($n = 5$)	0.090 ± 0.037
	TPer ($n = 3$)	0.650 ± 0.092
	Per ($n = 4$)	0.870 ± 0.130
Dorsal root	WT ($n = 5$)	0.316 ± 0.164
	TPer ($n = 3$)	0.590 ± 0.095
	Per ($n = 4$)	1.180 ± 0.057

20 μm of Triton X-100–insoluble fractions were fractionated on SDS-PAGE and stained with Coomassie blue. The OD corresponding to the peripherin and NF-L bands were then evaluated by densitometry. Ratios were calculated by dividing the peripherin OD by the NF-L OD for each mice. Results are mean ± SD.

the peripherin levels were increased by approximately fourfold in the ventral roots of TPer mice, approximately sevenfold in the ventral roots of Per mice, approximately twofold in dorsal roots of TPer mice, and approximately threefold in dorsal roots of Per mice. An analysis of cytoskeletal Triton-insoluble extracts from the brain and ventral roots revealed a recovery of peripherin in the insoluble fraction (Fig. 1 E). Densitometry of Coomassie blue–stained SDS-PAGE of Triton-insoluble extracts was further carried out to compare the peripherin levels to those of NF-L in ventral and dorsal root axons (Fig. 1 F and Table I). The identification of the bands corresponding to NF-M, NF-L, and peripherin was confirmed by Western blot analysis (Fig. 1 F). The results indicated that the levels of peripherin in ventral roots of transgenic mice overexpressing peripherin remained inferior to NF-L protein levels (Table I).

Extra Peripherin Causes Loss of Ventral Root Axons Late in Life

The peripherin transgenic mice developed normally and did not exhibit overt phenotypes and pathology until very late in life. A small number of mice from the TPer and Per lines were maintained for more than two years. After two years, the mice from both TPer and Per lines started to develop motor dysfunctions. Examination at microscopy and counting of L5 ventral roots revealed the loss of ~35% of motor axons in aged mice overexpressing peripherin when compared with their WT littermates (Fig. 2 and Table II). Note that axonal loss occurred predominantly in the ventral roots and that DRG axons were essentially spared. Unlike spinal motor neurons from WT mice (Fig. 2 C), most spinal motor neurons from transgenic mice were characterized by strong and diffuse peripherin immunoreactivity in their perikarya and neurites without evidence of

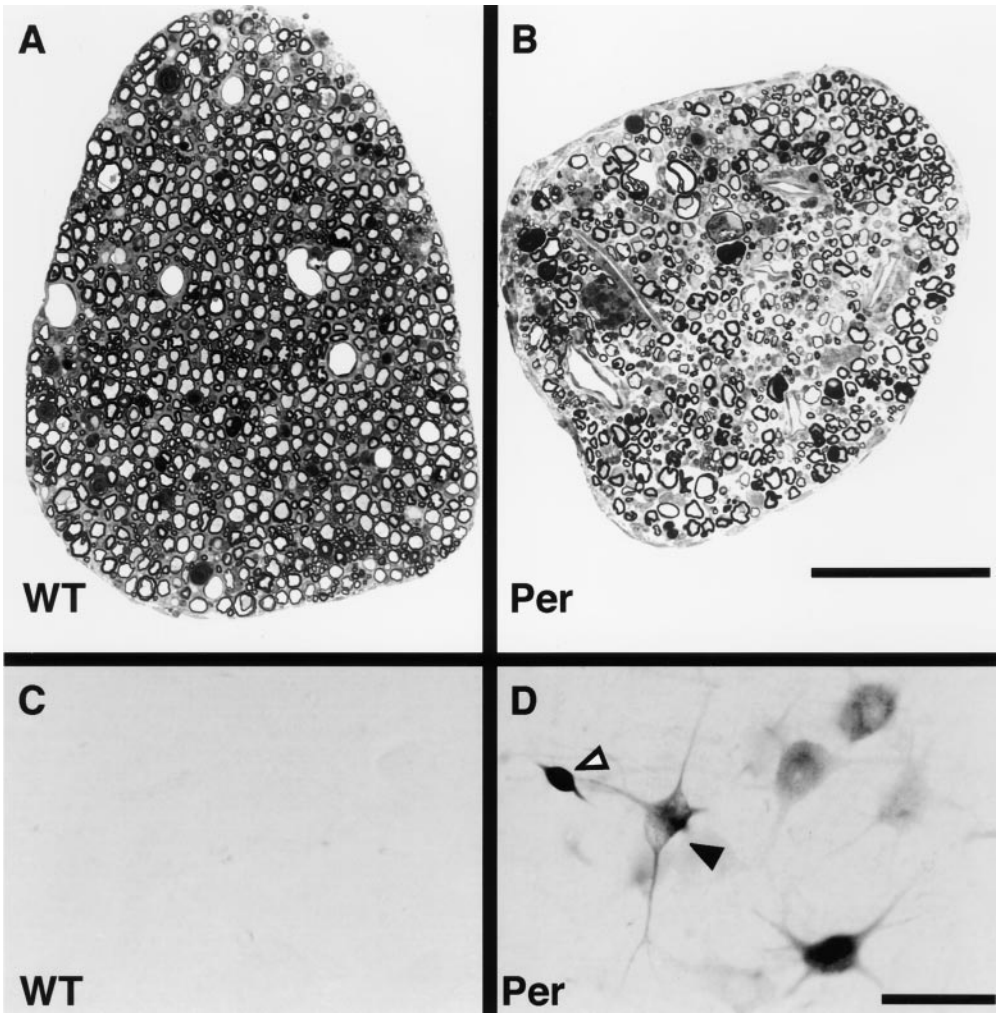

Figure 2. Motor axon degeneration and peripherin inclusions in aged mice overexpressing wild-type peripherin. (A and B) Toluidine blue staining of thin sections of L5 ventral root axons from 28-mo-old mouse littermates of WT (A) or Per (B) genotypes. (C and D) Immunohistochemical detection of peripherin in the spinal cord with a monoclonal antibody (NCL-Periph 1:200 dilution). No peripherin signal was detected in motor neurons of WT mice (C), whereas motor neurons of transgenic mice exhibited a strong diffuse labeling for peripherin in their perikarya (black arrowhead in D). Peripherin positive inclusions were also observed in neurites of spinal motor neurons (white arrowhead in D). Bars: (B) 100 μm; (D) 25 μm.

perikaryal swellings (Fig. 2 D). However, some peripherin inclusion bodies were observed in neurites especially in aged mice (Fig. 2 D).

Peripherin Overexpression in NF-L Null Background

Because substantial declines in NF-L gene expression occurs in ALS (Bergeron et al., 1994), we tested the effect of reducing NF-L levels on the progression of the peripherin-mediated disease. Mice of the TPer and Per lines were bred with our L−/− mice (Zhu et al., 1997) to obtain mice expressing the peripherin transgenes in a context of NF-L deficiency. The breeding resulted in the mendelian transmission of the peripherin transgenes and of the L−/− genotype.

Previous results obtained from cell culture studies and from L−/− mice (Beaulieu et al., 1999; Williamson et al., 1998) suggested that the organization of peripherin might be affected by the absence of NF-L. Western blot analysis of spinal cord extracts from the L−/−, Per;L−/−, and TPer;L−/− mice revealed reduced levels of peripherin, NF-H, and NF-M proteins as a consequence of NF-L deficiency (Fig. 3 A). Declines in levels of peripherin were also detected in the brain and optic nerve extracts from TPer;L−/− mice indicating that peripherin produced under the control of the Thy-1 promoter was also affected by the absence of NF-L (Fig. 3 A). Northern blot analysis of RNA from the brain and DRG of mice with various genotypes revealed that the NF-L disruption had no effects on peripherin mRNA levels (Fig. 3 B).

Table II. Number of Motor Axons in L5 Ventral Roots of Mice with Different Genotypes

Genotype	Age	Number of axons	Loss of motor axons
	mo		*%*
WT ($n = 3$)	6	1055 ± 64	0
WT ($n = 2$)	28	1069 ± 76	0
L−/− ($n = 3$)	6	860 ± 52	19
L−/− ($n = 3$)	20	918 ± 40	14
Per ($n = 2$)	6	1056 ± 45	0
Per ($n = 2$)	28	688 ± 87	35
TPer ($n = 3$)	6	1074 ± 54	0
TPer ($n = 1$)	28	684	35
Per;L−/− ($n = 3$)	6	567 ± 190	46
TPer;L−/− ($n = 2$)	2	741 ± 14	30
TPer;L−/− ($n = 3$)	6	563 ± 140	47
TPer;L−/− ($n = 3$)	14	438 ± 27	59

Loss of motor axons represents the percentage of missing axons as compared to WT. *n* represents the number of mice for each category. Results are mean ± SD.

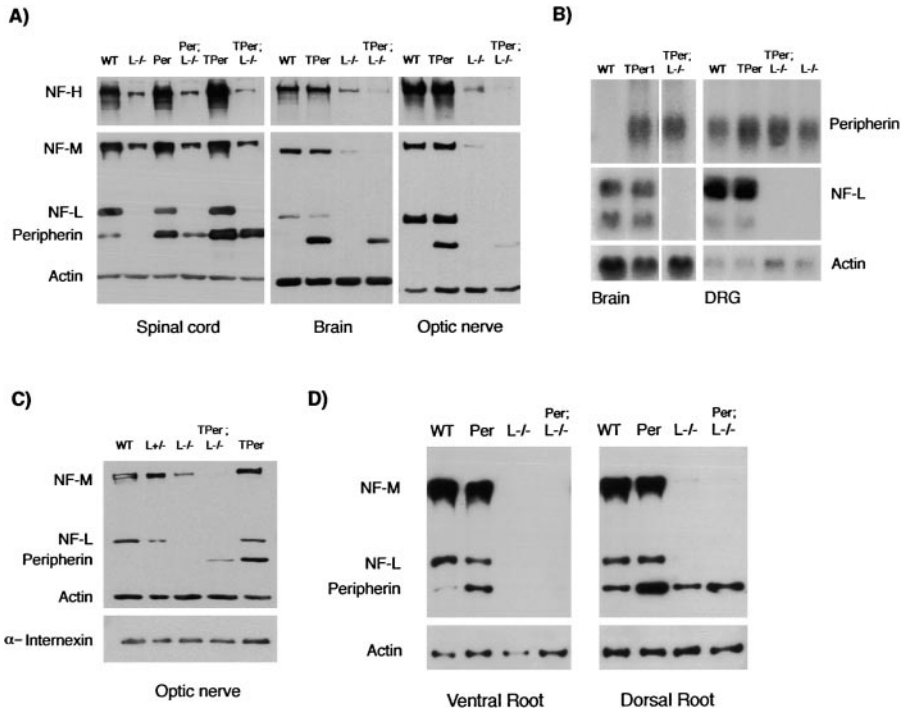

Figure 3. Reduced peripherin levels in absence of NF-L. (A) Western blot analysis of total protein extracts from the spinal cord, brain, and optic nerves of normal and transgenic 6-mo-old mice. The gels were loaded with 5 μg of protein from the brain and optic nerve or with 20 μg of protein from the spinal cord. Blots were incubated with a polyclonal antibody directed toward NF-H (top) or with a cocktail of monoclonal antibodies against NF-M, NF-L, peripherin, and actin (bottom). (B) Northern blot analysis of peripherin mRNA from the brain and DRG in the presence and absence of NF-L. The blots were hybridized with the peripherin probe, stripped, rehybridized with the NF-L probe, stripped again, and rehybridized with the actin probe. (C) Western blot analysis showing that α-internexin levels are not reduced in NF-L knockout mice. Duplicate gels were transferred to nitrocellulose membranes and incubated with either the monoclonal antibody cocktail as described above or with a polyclonal antibody against α-internexin. (D) Western blot of total protein extracts (5 μg) from ventral and dorsal roots of 4-mo-old mice showing that peripherin levels were less affected in dorsal roots than in ventral roots by the absence of NF-L.

In addition to NFs, CNS neurons express another type IV IF protein called α-internexin (Pachter and Liem, 1985). We have therefore examined the levels of α-internexin to test whether the downregulation of peripherin in NF-L null mice was due to a general destabilization of neuronal IF proteins. In contrast to peripherin, the levels of α-internexin were not affected by the absence of NF-L in L−/− and TPer;L−/− mice as revealed by Western blot analysis of optic nerve extracts (Fig. 3 C). Then we examined whether the peripherin levels in motor and sensory neurons were equally affected by the absence of NF-L (Fig. 3 D). Whereas peripherin was readily detected by Western blot in ventral root extracts of normal mice, the levels of peripherin and NF proteins were at exceedingly low levels in mice of the NF-L null background. It is noteworthy that the levels of peripherin were less affected by the absence of NF-L in dorsal roots than in ventral roots (Fig. 3 D). Electron microscopy of nondegenerating axons from ventral roots of 6-mo-old mice from the Per;L−/− and TPer;L−/− genotypes revealed that the cytoskeletal organization of these axons did not greatly differ from the one of motor axons of L−/− mice. In both cases there was a scarcity of IF structures with an elevated density of microtubules when compared with ventral root axons from mice of the WT and TPer genotypes (Fig. 4, A–D). In contrast to ventral root axons, small unmyelinated axons of dorsal roots in L−/− and TPer;L−/− mice showed little or no changes in the density of IF structures (Fig. 4, E–H). This observation is compatible with our Western blot result (Fig. 3 D) and with a report indicating that some unmyelinated sensory axons express peripherin in the absence of NFs (Goldstein et al., 1996).

NF-L Deficiency Accelerates Peripherin-mediated Disease

Mice with the TPer;L−/− and Per;L−/− genotypes developed aberrant hind limb positions and a progressive loss of hind limb mobility. This motor dysfunction was generally not apparent before 8 mo of age and often started on one side before spreading to the other side. In mice of both genotypes that were allowed to live until 14 mo of age, the progression of the phenotypes resulted in paralysis of the digits and of the lower limb articulations (Fig. 5 A). This phenotype prompted us to examine signs of dysfunction in younger mice. Thus, we measured the ability of 6-mo-old mice of different genotypes to grasp a vertical grid. This simple test revealed that the average grasping time for the TPer;L−/− mice was reduced by 80% when compared with mice with L−/−, TPer, or TPer;L+/− genotypes (Fig. 5 B).

Light microscopy of L5 dorsal roots from 6-mo-old animals showed no degenerating axons in L−/−, TPer;L−/−, and Per;L−/− mice (Fig. 6, A–C). In contrast, examination of the ventral roots revealed a massive degeneration of axons in the TPer;L−/− and Per;L−/− mice (Fig. 6, G and I) but not in the other types of mice that were examined at this age (Fig. 6, D, E, F, and H). Further examination of degenerating ventral roots by electron microscopy revealed the presence of degenerating myelin, axonal sproutings, and occasional axonal filamentous spheroids in the ventral roots of 6-mo-old Per;L−/− and TPer;L−/− mice (Fig. 6, J and K).

To evaluate the degree of degeneration, we counted the number of axons in the ventral roots of 6-mo-old mice of

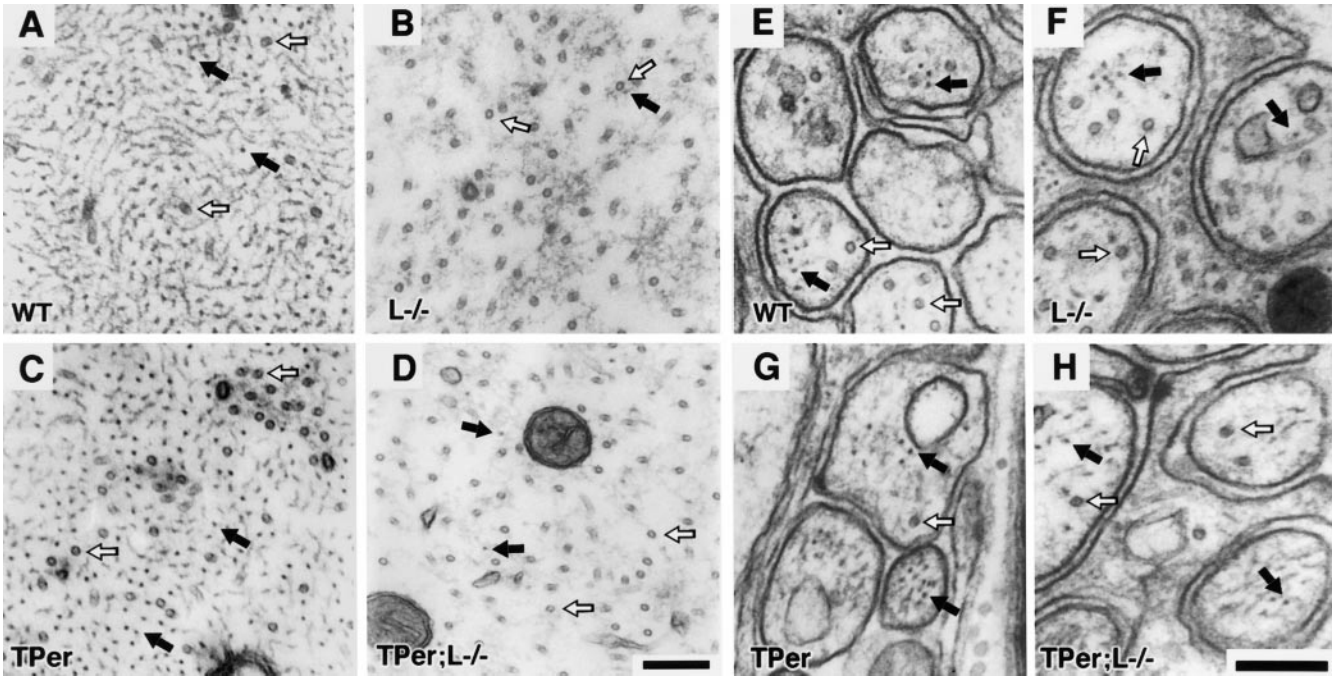

Figure 4. Peripherin does not substitute for NF-L. (A–D) Electron microscopy of large myelinated axons from the ventral root of WT (A), L−/− (B), TPer (C), and TPerL−/− (D) mice. Note the increased number of microtubules (white arrows) and the scarcity of IF structures (black arrows) in mice of L−/− and TPer;L−/− genotypes when compared with WT and TPer mice. (E–H) Electron microscopy of small unmyelinated axons from the dorsal root of either WT (E), L−/− (F), TPer (G), or TPer;L−/− (H) mice. Note that some of the null NF-L axons did not develop a scarcity of IF (black arrows). Bars, 0.2 μm.

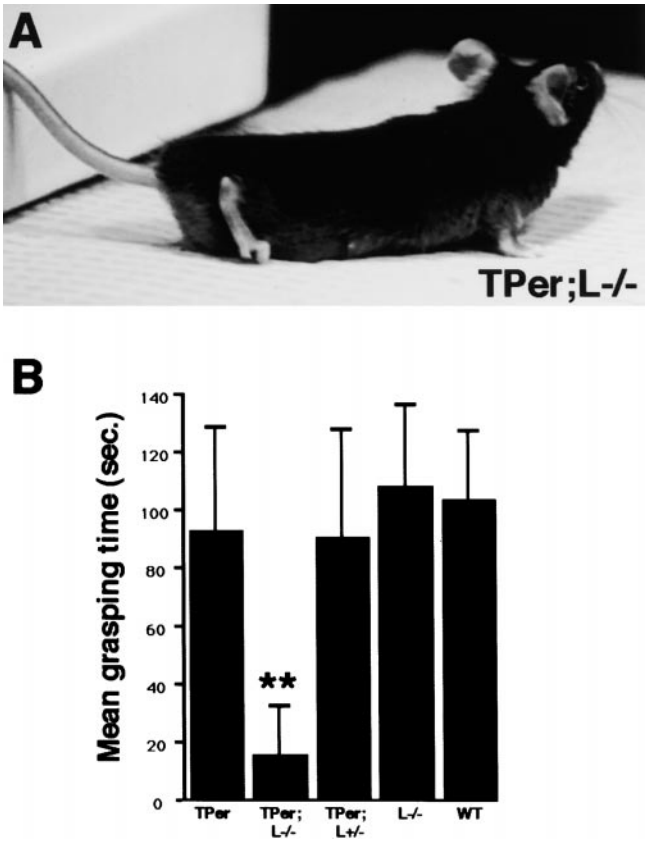

Figure 5. Motor dysfunction in NF-L null mice overexpressing peripherin. (A) Abnormal hind limb posture in a 14-mo-old TPer;L−/− mouse. (B) 6-mo-old TPer;L−/− mice have reduced grasping ability to a vertical grid. The results presented in the graphic are a mean from three separate tests performed on five mice of each genotype. Error bars correspond to standard deviations. **Indicates a significant difference from WT ($P < 0.01$) according to a Student's *t* test (unpaired, double tail).

different genotypes. The results are shown in Table II. The upregulation of peripherin alone did not affect the number of motor axons at this age, whereas the L−/− genotype was associated with a loss of ~16% of motor axons at both 6 and 20 mo of age. 6-mo-old mice overexpressing peripherin in NF-L null background exhibited declines of 45–50% in the number of their motor axons. The progressive nature of the overt phenotypes observed in TPer;L−/− and Per;L−/− mice prompted us to monitor the loss of motor axons in mice of different age. Analysis of ventral root axons in the TPer;L−/− mice at 2, 6, and 14 mo of age revealed a parallel increase of motor dysfunction and loss of motor axons culminating in the loss of 59% of motor axons in paralyzed mice at 14 mo of age (Table II).

To examine whether the massive loss of motor axons was accompanied by a corresponding death of neurons, we counted the number of motor neurons in a spinal cord region spanning a 3-mm rostral to caudal region at the level of L5 ventral roots. These counts were performed on Nissl-stained sections (Fig. 7). Two mice from each genotype were used for the analysis. Since similar results were obtained for the two mice of each genotype, the data were pooled and the mean number of large motor neuron per

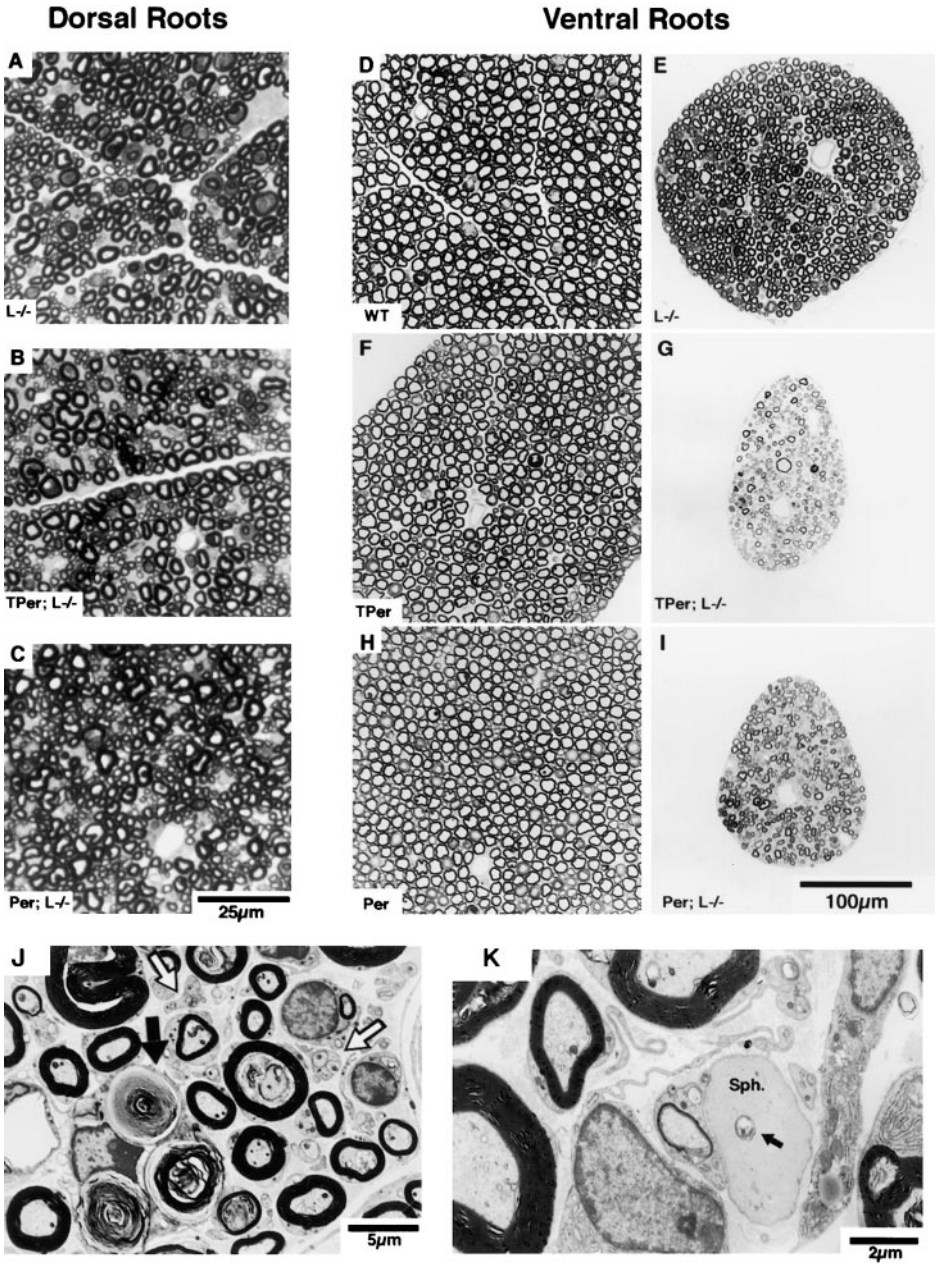

Figure 6. Accelerated degeneration of ventral root axons in mice overexpressing peripherin in absence of NF-L. (A–C) Toluidine blue staining of thin sections of L5 dorsal root axons from 6-mo-old L−/− (A), TPer;L−/− (B), and Per;L−/− (C) did not reveal degeneration of sensory axons in these mice. (D–H) No degeneration of axons was detected in L5 ventral roots of 6-mo-old WT (D), TPer (F), and Per (H) mice. The roots from 6-mo-old L−/− mice (E) were characterized by an atrophy of axons but did not contained degenerating axons. In contrast, massive degeneration of axons was evident in roots of 6-mo-old TPer;L−/− (G) and Per;L−/− (I) mice. (J and K) Electron microscopy of these same roots revealed the presence of degenerating axons (black arrow in J), axonal sproutings (white arrows in J), and axonal filamentous spheroids (sph in K) in ventral roots of the TPer;L−/− (J), and Per;L−/− (K) mice. The black arrow in K points to a mitochondria entrapped in an axonal spheroid. Bars: (A–C) 25 μm; (D–I) 100 μm; (J) 5 μm; (K) 2 μm.

ventral horn was calculated (Table III). This analysis revealed a dramatic reduction in the mean number of large spinal motor neurons (64% neuronal loss) present in the ventral horns of 14-mo-old TPer;L−/− mice as compared with normal, TPer, and L−/− mice (Fig. 7 and Table III). Moreover, the loss of motor neurons during aging of the TPer;L−/− mice was progressive since 5-mo-old mice showed a lower degree of neuronal loss (Table III).

We then verified whether an increased abundance of peripherin inclusions was associated with the acceleration of the peripherin-mediated disease in the absence of NF-L. A very weak peripherin immunostaining was observed in spinal motor axons of WT and L−/− mouse using an anti-peripherin monoclonal antibody (Fig. 8 A). In TPer and Per transgenic mice having a wild-type NF-L background, a generally diffused peripherin staining with the occasional presence of peripherin inclusion bodies was observed in spinal motor neurons (Figs. 8 B and 2 D). Peripherin inclusions were more frequent in the proximal axons of motor neurons of TPer;L+/− and Per;L+/− mice (Fig. 8 C). Finally, the spinal cord of the TPer;L−/− and Per;L−/− mice was characterized by the presence of abundant peripherin inclusions in the perikarya and axons of motor neurons and by a general disappearance of diffuse peripherin staining (Fig. 8, D and E). Similar peripherin inclusions were also observed in the motor nucleus of the facial and trigeminal nerves, in the nucleus ambiguous, in large DRG neurons, and in the mesencephalic trigeminal nucleus of the TPer;L−/− and Per;L−/− mice (data not shown). In the TPer;L−/− mice, the peripherin inclusions were detectable in spinal motor neurons of mice at 2, 6, and 14 mo of age. In thin sections stained with Toluidine

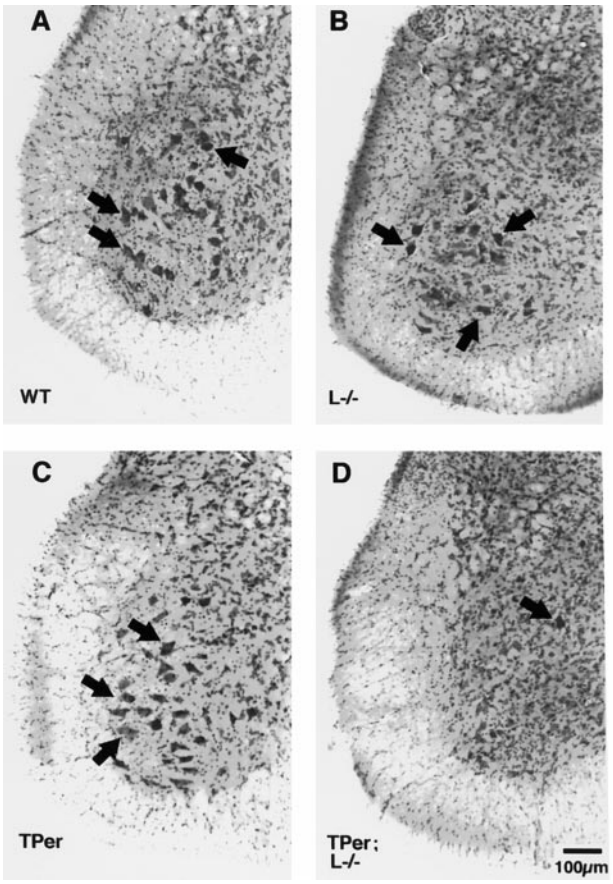

Figure 7. Cresyl violet staining of L5 spinal cords. Light microscopy of spinal cords from 14-mo-old WT, L−/−, TPer, and TPer; L−/− mice showed a marked loss of large motor neurons (arrows) in TPer;L−/− mice.

blue, the peripherin inclusions appeared as hyaline inclusion bodies with sizes ranging from 2 to 30 μm in length (Fig. 8 F). Multiple distinct inclusion bodies were often detected within the same neuron. These inclusions never filled completely the perikarya of motor neurons. At electron microscopy, the peripherin inclusions appeared as disorganized accumulations of 10-nm filaments mingled with various membranous residues (Fig. 8, G and H). Inclusion bodies containing mitochondria were also frequently observed (Fig. 8 H).

Table III. Number of Large Motor Neurons per Ventral Horn in L5 Spinal Cord Sections

Genotype	Age	Mean number of motor neurons per ventral horn	Loss of motor neurons
	mo		*%*
WT (n = 103)	14	19.9 ± 4.8	0
TPer (n = 115)	14	21.4 ± 5.1	0
L−/− (n = 110)	14	15.9 ± 4.2	20
TPer;L−/− (n = 74)	5	11 ± 3.8	45
TPer;L−/− (n = 148)	14	7.3 ± 4.4	64

Loss of motor axons represents the percentage of missing axons as compared to WT. n represents the number of ventral horn sections for each category. Results are mean ± SD.

Detection of NF-M and NF-H in Peripherin Inclusions

Since cell culture studies indicated that the large NF subunits can have a destabilizing effect on the organization of peripherin (Beaulieu et al., 1999), we examined whether the NF-M or NF-H proteins were present in the peripherin inclusion bodies. Double indirect immunofluorescence was carried out on spinal cord sections from the TPer;L−/− mice using a peripherin polyclonal antibody and different monoclonal antibodies against NF-M or NF-H proteins. All peripherin inclusions observed in these analysis were immunoreactive for NF-M, as revealed by the NN-18 antibody (Fig. 8 I), and for dephosphorylated NF-H as revealed by the SMI-32 antibody (Fig. 8 J). A majority of inclusions also contained hyperphosphorylated NF-H as revealed by their immunoreactivity to the RT-97 antibody (Fig. 8 K). In rare cases, motor neurons showed a diffuse pattern of peripherin staining in their perikarya. One such neuron was encountered in the course of a double labeling experiment involving the anti–NF-M monoclonal antibody. It is noteworthy that this neuron, which lacked inclusion bodies, was also showing a really weak NF-M immunoreactivity (Fig. 8 L) suggesting that the formation of peripherin aggregates in motor neurons requires the presence of the large NF subunits.

Early Detection of Peripherin Inclusions in Mice Bearing SOD1^{G37R}

Taken together, our results and the previous reports that peripherin is present in the majority of IF inclusions in sporadic ALS cases (Corbo and Hays, 1992; Migheli et al., 1993; Tu et al., 1996) suggest that peripherin may play a contributory role in ALS pathogenesis. Further support for this view came from our immunodetection of peripherin inclusions in spinal cord sections of paralyzed and presymptomatic mice expressing a Glycine 37 to Arginine mutant form of SOD1 (SOD1^{G37R}) associated with familial human ALS (Wong et al., 1995). This analysis was carried out in two different lines of transgenic mice, lines 42 and 29, which are characterized by disease onset at ~5 and ~11 mo, respectively. Staining of spinal cord sections from normal mice did not show any peripherin inclusions but allowed the detection of peripherin in axons from the dorsal column and in some motor axons of the ventral horns (Fig. 9, A and E). In contrast, peripherin inclusion bodies were observed in paralyzed mice from both SOD1^{G37R} lines (Fig. 9, B and D). Staining of sections from presymptomatic mice of line 29 revealed the presence of peripherin inclusions in 5-mo-old mice (Fig. 9 C). Similar inclusions were also observed in one out of three mice studied at 3 mo of age, indicating that the formation of peripherin inclusions in motor axons occurs at an early stage of the disease. It is noteworthy that peripherin inclusions were also detected in the dorsal column in paralyzed but not in presymptomatic mice from both SOD1^{G37R} lines (Fig. 9, F–H).

Discussion

The transgenic mouse models described here are the first examples of extensive motor neuron death in mice caused by an upregulation of a wild-type IF protein. There are previous reports of neuronal death due to expression of IF

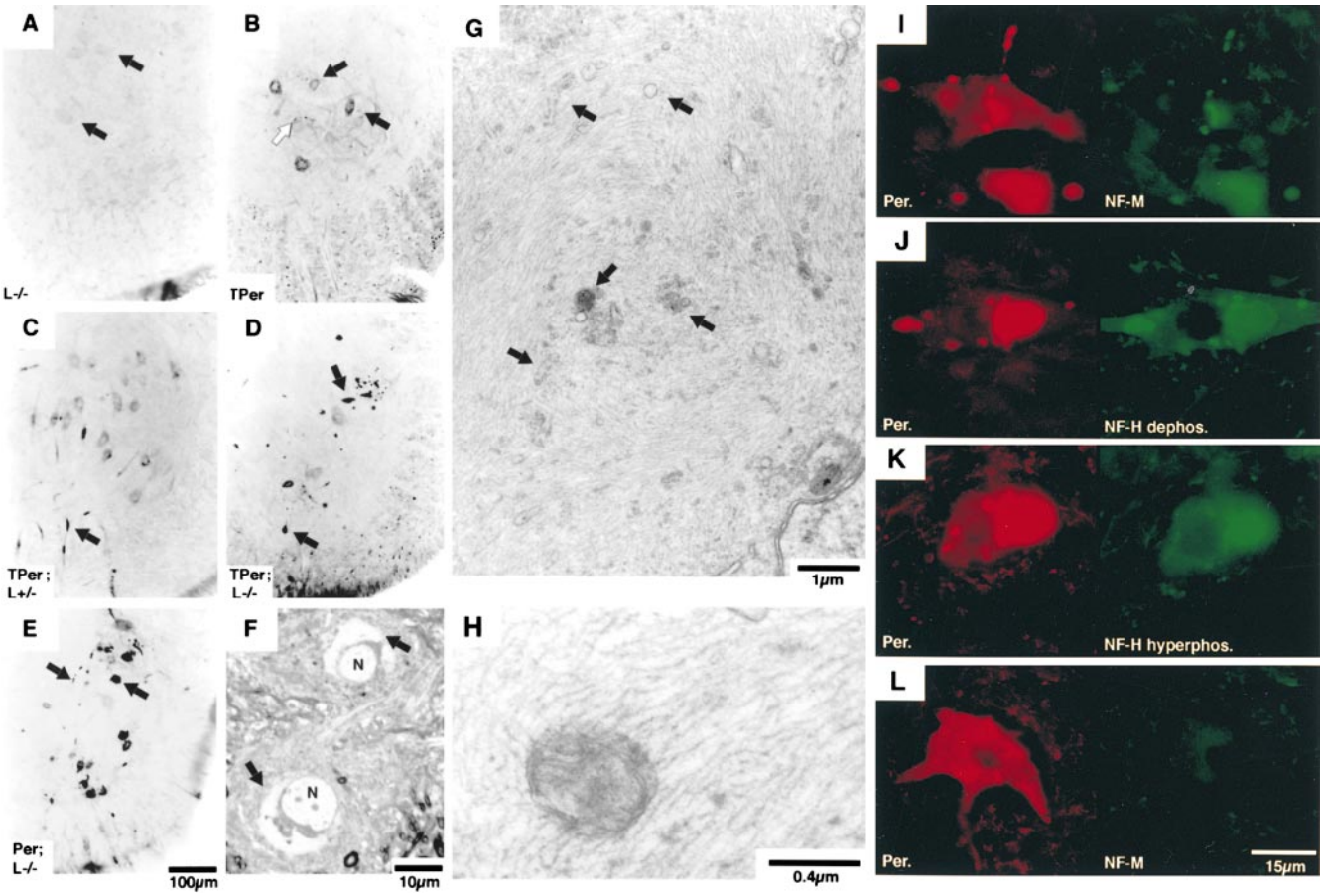

Figure 8. IF inclusions contain peripherin and NF proteins. (A–E) Immunohistochemical detection of peripherin in spinal cord samples with a monoclonal antibody (NCL-Periph 1:200 dilution). (A) A very weak peripherin signal was detected in motor neurons (black arrows in A) of NF-L −/− mice. (B) In the TPer mice, diffuse peripherin labeling (black arrow) and some small inclusions (white arrow) were detected in motor neurons. (C) The lack of 50% of NF-L in the TPer;L +/− mice caused the formation of more frequent peripherin inclusions in motor neuron axons (black arrow). (D and E) The total absence of NF-L resulted in the disappearance of a diffuse peripherin staining and in the formation of numerous peripherin inclusions in the cell bodies and axons of spinal motor neurons (black arrows) of TPer and Per mice. (F) Hyaline inclusion bodies (black arrow) in the cytoplasm of motor neurons detected by Toluidine blue staining of thin sections of the spinal cord from TPer;L −/− mice. N indicates the cell nucleus. (G and H) Electron microscopy of inclusion bodies found in motor neurons of TPer;L −/− (G) and PerL −/− (H) mice. The inclusions are formed of 10-nm filaments that are sequestering membranous material (black arrows in G) and mitochondria (H). (I–L) Double indirect immunofluorescence of motor neurons from the spinal cord of TPer;L −/− mice. A polyclonal anti-peripherin antibody (AB1530 1:1,000 dilution) in red and the various monoclonal antibodies directed against NF-M (NN-18 1:100 dilution), dephosphorylated NF-H (SMI-32 1:500 dilution) or hyperphosphorylated NF-H (RT 97 1:500 dilution) in green reveal the colocalization of peripherin, NF-M (I) and NF-H (J and K) in the inclusion bodies. A double immunofluorescence staining of one neuron showing a diffused peripherin staining (L) in absence of immunoreactivity for NF-M. All results presented in this figure were obtained from 6–8-mo-old mice. Bars: (A–E) 100 μm; (F) 110 μm; (G) 1 μm; (H) 0.4 μm; (I–L) 15 μm.

transgenes (Lee et al., 1994; Tu et al., 1997; Ching et al., 1999; Ma et al., 1999), but this is the first example of massive and selective motor neuron death due to high levels of wild-type IF protein. Our results demonstrate that an upregulation of wild-type peripherin is sufficient to induce selective motor neuron death during aging and that a deficiency of NF-L is a factor that precipitates dramatically the onset and progression of disease, probably through the deleterious effects of NF-M and NF-H on peripherin organization. Moreover, the acceleration of disease correlated with the frequency of IF inclusions containing peripherin in spinal motor neurons.

Three independent studies have shown that peripherin is present in a majority of IF inclusions in ALS patients (Corbo and Hays, 1992; Migheli et al., 1993; Tu et al., 1996). We have also detected similar inclusions in presymptomatic mice expressing a mutant $SOD1^{G37R}$ linked to familial ALS (Fig. 9). Such IF inclusions in ALS may occur as a consequence of axonal transport defects (Zhang et al., 1997; Williamson and Cleveland, 1999). Alternatively, the results presented here and the intense immunoreactivity of IF inclusions for peripherin in ALS make it plausible that such inclusion bodies could originate from an upregulation of peripherin occurring at the level of gene transcription. Peripherin is normally expressed at low levels in motor neurons (Troy et al., 1990a), but enhanced levels,

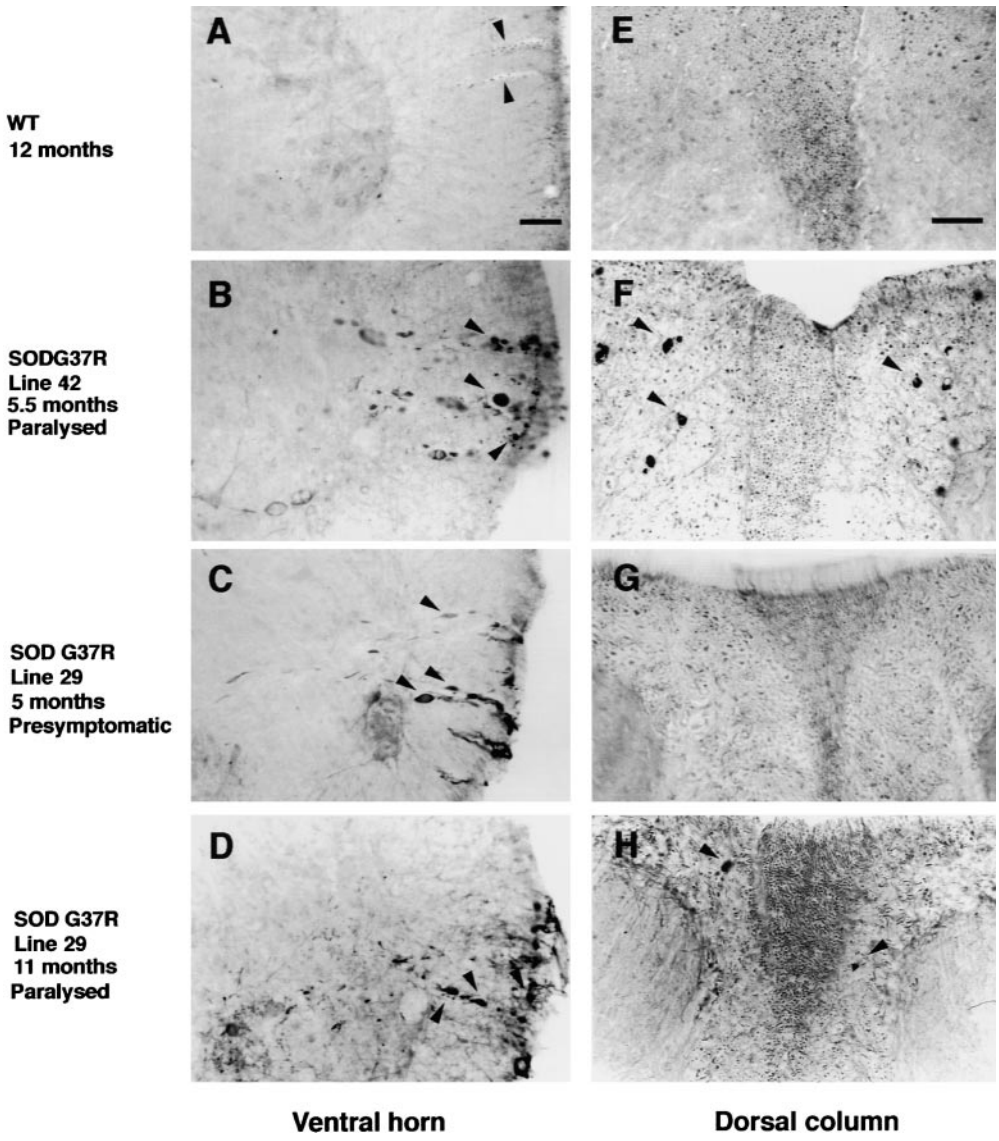

Figure 9. Peripherin inclusions in SOD1^{G37R} mice. Immunohistochemical labeling with a peripherin polyclonal antibody (AB1530 1:1,000 dilution) revealed the presence of peripherin-containing inclusions in motor axons of mice expressing the mutant SOD1^{G37R}, at early stage (arrowheads in C), and end stage of disease (arrowheads in B and D). Staining from spinal cord sections of normal mice yielded a weak staining for peripherin in ventral horn axons (arrowhead in A) and dorsal column axons (E) but no peripherin inclusions were detected. Note the detection of peripherin inclusions in the dorsal column at end stage of disease in mice from line 42 and line 29 (arrowhead in F and H). Bars: (A–D) 75 μm; (E–H) 50 μm.

and perhaps IF inclusion formation, could be part of a regenerative response observed in ALS. It is well established that after nerve injury the levels of peripherin mRNA are induced by three- to fourfold in motor neurons (Troy et al., 1990a). Other genes associated with the regenerative response after neuronal injury, such as GAP43 and α1-tubulin, have been reported to be upregulated in ALS (Parhad et al., 1992). Moreover, peripherin is upregulated by cytokines such as IL-6 and LIF (Djabali et al., 1993; Sterneck et al., 1996). There is growing evidence for an involvement of inflammatory reactions in ALS that could account for enhanced levels of peripherin. A recent study has indicated an increase of IL-6 in the cerebrospinal fluid of ALS patient (Sekizawa et al., 1998). Moreover, an upregulation of LIF has been reported in an in vivo model of glutamate excitotoxicity (Kurek et al., 1998), which is another hypothesized mechanism of toxicity associated with ALS (Lin et al., 1998). Finally, inflammatory cytokines are associated with astrogliosis, which is a common phenomenon in ALS and in other neurodegenerative diseases (Klein et al., 1997).

Our previous cell culture studies with peripherin and NF cDNA clones in SW13 cells demonstrated that peripherin can self-assemble to form an IF network and that it assembles with the NF network in the presence of NF-L (Beaulieu et al., 1999). However, in absence of NF-L, the NF-M and NF-H proteins interact with peripherin to form disorganized IF structures (Beaulieu et al., 1999). Perhaps, this could explain why the peripherin-mediated disease was exacerbated in the NF-L null background. The increased number of IF inclusion bodies in mice deficient for NF-L is probably due to abnormal interactions of peripherin and the high molecular mass NF subunits. In this regard, it is noteworthy that rare motor neurons in TPer;L−/− mice that were devoid of NF-M protein did not develop IF inclusions bodies even though peripherin was detected at elevated levels (Fig. 8 L). Similarly, small sensory neurons that express peripherin but are devoid of NFs (Ferri et al., 1990; Goldstein et al., 1996) maintained a normal IF network in the NF-L null background (Fig. 4).

The NF-L null background mimics in part the depletion in NF-L mRNA levels occurring in motor neurons of ALS

patients. In situ hybridization studies revealed a striking 60% reduction of NF-L mRNA levels in the α-motor neurons of ALS patients as compared with age-matched controls (Bergeron et al., 1994). Moreover, greater declines in NF-L mRNA levels (87%) were detected in motor neurons having spheroids or perikaryal filamentous accumulations (Bergeron et al., 1994). Remarkably, our data demonstrate that a partial depletion in NF-L levels is sufficient to increase the abundance of peripherin inclusions. A 50% reduction of NF-L mRNA in the TPer;L+/− and Per;L+/− mice resulted in the formation of peripherin inclusions in proximal axons of motor neurons (Fig. 8 C)

The formation of IF inclusions in motor neurons has been associated with motor dysfunction in three other types of transgenic mice (Côté et al., 1993; Xu et al., 1993; Lee et al., 1994). However, the properties of IF inclusions described here differ in several aspects from those of IF inclusions observed in mice overexpressing NF transgenes. Whereas large perikaryal NF accumulations excluding other cytoplasmic material were observed in the NF-H and NF-L transgenic mice (Côté et al., 1993; Xu et al., 1993), the inclusion bodies found in peripherin transgenic mice are relatively small, they contain membranous material including mitochondria and they occur in both cell bodies and axons. Because of their size and axonal localization, the inclusions observed in peripherin transgenic mice are more similar to the IF inclusions found in human ALS (reviewed in Chou, 1995) and in mutant SOD1 transgenic mice than are the NF swellings observed in the NF transgenic mice. More importantly, unlike mice overexpressing wild-type NF proteins (Côté et al., 1993; Xu et al., 1993; our unpublished observation), the mice with peripherin inclusions exhibited axonal degeneration and massive death of motor neurons.

Unexpectedly, the results shown here demonstrate that the presence of NF-L is not required for the formation of IF inclusions in motor neurons. This is an important finding because an involvement for NF proteins in ALS has been recently challenged by studies with L−/− mice and NF-H/lacZ mice showing that the absence of intact NFs in axons did not prevent SOD1-mediated disease (Williamson et al., 1998; Eyer et al., 1998). This led to the belief that IF proteins play a minor role in ALS pathogenesis, a notion that must be reexamined at the light of our results showing that disorganized IF structures containing high molecular weight NF proteins together with peripherin can provoke motor neuron death in absence of NF-L.

The exact mechanism underlying cell death by such IF inclusion bodies remains to be elucidated. A block of intracellular transport by multiple IF inclusions in the axon is a possible mechanism that may contribute to neurodegeneration and perhaps cell death in the peripherin transgenic mice described here. Alternatively, the peripherin-containing inclusions could provoke neurodegeneration by the sequestration of organelles such as mitochondria (Fig. 8) or other components essential for cell survival. Such a mechanism has been postulated to explain the toxicity of SOD1 aggregates detected in SOD1 mutant mice (Bruijn et al., 1998). In fact, there is growing evidence for protein aggregation as a common etiology in neurodegenerative disorders including ALS, Alzheimer's disease, prion disease, Parkinson's disease, and a class of disorders caused by expanded CAG repeats encoding polyglutamines (for review see Kakizuka, 1997). The general working hypothesis is that mutations in proteins may result in misfolding and decreased protein degradation, leading to disturbance in homeostatic mechanisms. For instance, an upregulation of proteins with chaperoning activity was found to protect against aggregation of mutant ataxin-1 (Cummings et al., 1998) and also from the toxicity of SOD1 mutants (Bruening et al., 1998). Recently, polyglutamine domain proteins derived from expanded CAG repeats were found to bind specifically to NF-L and to alter NF network (Nagai et al., 1999). The data presented here introduces a novel concept in that no mutant proteins are required for the development of inclusion bodies. In future studies it would be of interest to investigate whether peripherin inclusions can also be derived by posttranslational modifications of IF proteins. It is well documented that changes in phosphorylation can alter the assembly properties of NF proteins (for review see Julien and Mushynski, 1998). In addition, the nitration of tyrosine residues in the NF-L protein, a phenomenon that may occur in ALS (Crow et al., 1997), could impair its assembly and perhaps would favor interactions of peripherin with the high-molecular mass NF subunits to form noxious IF inclusions.

In conclusion, our study demonstrates for the first time that an upregulation of wild-type peripherin can cause the selective death of motor neurons during aging and that a NF-L deficiency is a factor that precipitates the disease. These results combined with the specific detection of peripherin inclusions in motor neurons of sporadic ALS cases (Corbo and Hays, 1992; Migheli et al., 1993; Tu et al., 1996) and in motor neuron neurons of presymptomatic $SOD1^{G37R}$ mice (Fig. 9) provide compelling evidence for a potential role of peripherin in ALS pathogenesis.

The technical assistance of P. Hince, D. Houle, and G. Gagnon is gratefully acknowledged. We also thank J. Robertson, W.E. Mushynski, and J.S. Couillard-Després.

This research was supported by the Medical Research Council of Canada (MRC), the ALS association (USA), and the ALS society of Canada. J.-M. Beaulieu is a recipient of studentships from the Natural Science and Engineering Research Council of Canada (NSERC), from Le Fond de Recherche en Santé du Québec (FRSQ) and from the McDonald Stewart Foundation. M.D. Nguyen was a recipient of a MRC studentship. J.-P. Julien has a MRC Senior Scholarship.

Submitted: 4 June 1999
Revised: 23 September 1999
Accepted: 24 September 1999

References

Athlan, E.S., and W.E. Mushynski. 1997. Heterodimeric associations between neuronal intermediate filament proteins. *J. Biol. Chem.* 272:31073–31078.

Bancroft, J.D., and A. Stevens. 1990. Theory and practice of histological techniques. 3rd edition. Churchill Livingstone, Inc. New York, NY. 726 pp.

Beaulieu, J.M., J. Robertson, and J.P. Julien. 1999. Interactions between peripherin and neurofilaments in cultured cells: disruption of peripherin assembly by the NF-M and NF-H subunits. *Biochem. Cell Biol.* 77:41–45.

Bergeron, C., K. Beric-Maskarel, S. Muntasser, L. Weyer, M.J. Somerville, and M.E. Percy. 1994. Neurofilament light and polyadenylated mRNA levels are decreased in amyotrophic lateral sclerosis motor neurons. *J. Neuropathol. Exp. Neurol.* 53:221–230.

Brinster, R.L., H.Y. Chen, M. Trumbauer, A.W. Senear, R. Warren, and R.D. Palmiter. 1981. Somatic expression of herpes thymidine kinase in mice following injection of a fusion gene into eggs. *Cell.* 27:223–231.

Brody, B.A., C.A. Ley, and L.M. Parysek. 1989. Selective distribution of the 57

kDa neural intermediate filament protein in the rat CNS. *J. Neurosci.* 9:2391–2401.

Bruening, W., B. Giasson, W. Mushynski, and H.D. Durham. 1998. Activation of stress-activated MAP protein kinases up-regulates expression of transgenes driven by the cytomegalovirus immediate/early promoter. *Nucleic Acids Res.* 26:486–489.

Bruijn, L.I., M.K. Houseweart, S. Kato, K.L. Anderson, S.D. Anderson, E. Ohama, A.G. Reaume, R.W. Scott, and D.W. Cleveland. 1998. Aggregation and motor neuron toxicity of an ALS-linked SOD1 mutant independent from wild-type SOD1. *Science.* 281:1851–1854.

Bruijn, L.I., M.W. Becher, M.K. Lee, K.L. Anderson, N.A. Jenkins, N.G. Copeland, S.S. Sisodia, J.D. Rothstein, D.R. Borchelt, D.L. Price, and D.W. Cleveland. 1997. ALS-linked SOD1 mutant G85R mediates damage to astrocytes and promotes rapidly progressive disease with SOD1-containing inclusions. *Neuron.* 18:327–338.

Carpenter, S. 1968. Proximal axonal enlargement in motor neuron disease. *Neurology*. 18:841–851.

Ching, G.Y., and R.K.H. Liem. 1993. Assembly of type IV neuronal intermediate filaments in nonneuronal cells in the absence of preexisting cytoplasmic intermediate filaments. *J. Cell Biol.* 122:1323–1335.

Ching, G.Y., C.L. Chien, R. Flores, and R.K. Liem. 1999. Overexpression of alpha-internexin causes abnormal neurofilamentous accumulations and motor coordination deficits in transgenic mice. *J. Neurosci*. 19:2974–2986.

Chou, S.M. 1995. Pathology of motor system disorder. *In* Motor Neuron Disease: Biology and Management. P.N. Leigh and M. Swash, editors. Springer-Verlag, London. 53–92.

Corbo, M., and A.P. Hays. 1992. Peripherin and neurofilament protein coexist in spinal spheroids of motor neuron disease. *J. Neuropathol. Exp. Neurol.* 51: 531–537.

Côté, F., J.F. Collard, and J.-P. Julien. 1993. Progressive neuropathy in transgenic mce expressing the human neurofilamen heavy gene: a mouse model of amyotrophic lateral sclerosis. *Cell.* 73:35–46.

Crow, J.P., Y.Z. Ye, M. Strong, M. Kirk, S. Barnes, and J.S. Beckman. 1997. Superoxide dismutase catalyzes nitration of tyrosines by peroxynitrite in the rod and head domains of neurofilament-L. *J. Neurochem.* 69:1945–1953.

Cui, C., P.J. Stambrook, and L.M. Parysek. 1995. Peripherin assembles into homopolymers in SW13 cells. *J. Cell Sci.* 108:3279–3284.

Cummings, C.J., M.A. Mancini, B. Antalffy, D.B. DeFranco, H.T. Orr, H.Y. Zoghbi. 1998. Chaperone suppression of aggregation and altered subcellular proteasome localization imply protein misfolding in SCA1. *Nature Genet.* 19:148–154.

Djabali, K., A. Zissopoulou, M.J.D. Hoop, S.D. Georgatos, and C.G. Dotti. 1993. Peripherin expression in hippocampal neurons induced by muscle soluble factors. *J. Cell Biol.* 123:1197–1206.

Escurat, M., K. Djabali, M. Gumpel, F. Gros, and M.M. Portier. 1990. Differential expression of two neuronal intermediate-filament proteins, peripherin and the low-molecular-mass neurofilament protein NF-L during the development of the rat. *J. Neurosci.* 10:764–784.

Eyer, J., D.W. Cleveland, P.C. Wong, and A.C. Peterson. 1998. Pathogenesis of two axonopathies does not require axonal neurofilaments. *Nature.* 391:584–587.

Feinberg, A.P., and B. Vogelstein. 1983. A technique for radiolabeling DNA restriction endonuclease fragments to high specific activity. *Anal. Biochem*. 132:6–13.

Ferri, G.L., A. Sabani, L. Abelli, J.M. Polak, D. Dahl, and M.M. Portier. 1990. Neuronal intermediate filaments in rat dorsal root ganglia: differential distribution of peripherin and neurofilament protein immunoreactivity and effect of capsaicin. *Brain Res.* 515:331–335.

Goldstein, M.E., P. Grant, S.B. House, D.B. Henken, and H. Gainer. 1996. Developmental regulation of two distinct neuronal phenotypes in rat dorsal root ganglia. *Neuroscience.* 71:243–258.

Gurney, M.E., H. Pu, A.Y. Chiu, M.C. Dal Canto, C.Y. Polchow, D.D. Alexander, J. Caliendo, A. Hentati, Y.W. Kwon, H.X. Deng, et al. 1994. Motor neuron degeneration in mice that express a human Cu,Zn superoxide dismutase mutation. *Science.* 264:1772–1775.

Ho, C.L., S.S.M. Chin, K. Carnevale, and R.K.H. Liem. 1995. Translation initiation and assembly of peripherin in cultured cells. *Eur. J. Cell Biol.* 68:103–112.

Jacomy, H., and O. Bosler. 1995. Catecholaminergic innervation of the suprachiasmatic nucleus in the adult rat: ultrastructural relationships with neurons containing vasoactive intestinal peptide or vasopressin. *Cell Tissue Res.* 280: 87–96.

Julien, J.P., and W.E. Mushynski. 1998. Neurofilaments in health and disease. *Prog. Nucleic Acid Res. Mol. Biol.* 61:1–23.

Kakizuka, A. 1997. Degenerative ataxias: genetics, pathogenesis and animal models. *Curr. Opin. Neurol.* 10:285–290.

Kato, S., M. Shimoda, Y. Watanabe, K. Nakashima, K. Takahashi, and E. Ohama. 1996. Familial amyotrophic lateral sclerosis with a two base pair deletion in superoxide dismutase 1: gene multisystem degeneration with intracytoplasmic hyaline inclusions in astrocytes. *J. Neuropathol. Exp. Neurol.* 55: 1089–1101.

Klein, M.A., J.C. Moller, L.L. Jones, H. Bluethmann, G.W. Kreutzberg, and G. Raivich. 1997. Impaired neuroglial activation in interleukin-6 deficient mice. *Glia.* 19:227–233.

Kurek, J.B., T.M. Bennett, J.J. Bower, C.M. Muldoon, and L. Austin. 1998. Leukaemia inhibitory factor (LIF) production in a mouse model of spinal trauma. *Neurosci. Lett.* 249:1–4.

Lecomte, M.J., M. Basseville, F. Landon, V. Karpov, and M. Fauquet. 1998. Transcriptional activation of the mouse peripherin gene by leukemia inhibitory factor: involvement of STAT proteins. *J. Neurochem*. 70:971–982.

Lee, M.K., Z. Xu, P.C. Wong, and D.W. Cleveland. 1993. Neurofilaments are obligate heteropolymers in vivo. *J. Cell Biol.* 122:1337–1350.

Lee, M.K., J.R. Marszalek, and D.W. Cleveland. 1994. A mutant neurofilament subunit causes massive, selective motor neuron death: implications for the pathogenesis of human motor neuron disease. *Neuron.* 13:975–988.

Lin, C.L., L.A. Bristol, L. Jin, M. Dykes-Hoberg, T. Crawford, L. Clawson, and J.D. Rothstein. 1998. Aberrant RNA processing in a neurodegenerative disease: the cause for absent EAAT2, a glutamate transporter, in amyotrophic lateral sclerosis. *Neuron.* 20:589–602.

Ma, D., L. Descarries, K.D. Micheva, Y. Lepage, J.-P. Julien, and G. Doucet. 1999. Severe neuronal losses with age in the parietal cortex and ventrobasal thalamus of mice transgenic for the human NF-L neurofilament protein. *J. Comp. Neurol.* 406:433–448.

Migheli, A., T. Pezzulo, A. Attanasio, and D. Schiffer. 1993. Peripherin immunoreactive structures in amyotrophic lateral sclerosis. *Lab. Investig.* 68:185–191.

Muma, N.A., P.N. Hoffman, H.H. Slunt, M.D. Applegate, I. Lieberburg, and D.L. Price. 1990. Alterations in levels of mRNAs coding for neurofilament protein subunits during regeneration. *Exp. Neurol.* 107:230–235.

Nagai, Y., O. Onodera, J. Chun, W.J. Strittmatter, and J.R. Burke. 1999. Expanded polyglutamine domain proteins bind neurofilament and alter the neurofilament network. *Exp. Neurol.* 155:195–203.

Pachter, J.S., and R.K. Liem. 1985. alpha-Internexin, a 66-kD intermediate filament-binding protein from mammalian central nervous tissues. *J. Cell Biol.* 101:1316–1322.

Parhad, I.M., R. Oishi, and A.W. Clark. 1992. GAP-43 gene expression is increased in anterior horn cells of amyotrophic lateral sclerosis. *Ann. Neurol.* 31:593–597.

Parysek, L.M., and R.D. Goldman. 1988. Distribution of a novel 57 kDA intermediate filament IF protein in the nervous system. *J. Neurosci.* 8:555–563.

Parysek, L.M., M.A. McReynolds, R.D. Goldman, and C.A. Ley. 1991. Some neural intermediate filaments contain both peripherin and the neurofilament proteins. *J. Neurosci. Res.* 30:80–91.

Ripps, M.E., G.W. Huntley, P.R. Hof, J.H. Morrison, and J.W. Gordon. 1995. Transgenic mice expressing an altered murine superoxide dismutase gene provide an animal model of amyotrophic lateral sclerosis. *Proc. Natl. Acad. Sci. USA*. 92:689–693.

Rosen, D.R., T. Siddique, D. Patterson, D.A. Figlewicz, P. Sapp, A. Hentati, D. Donaldson, J. Goto, J.P. O'Regan, H.X. Deng, et al. 1993. Mutations in Cu/Zn superoxide dismutase gene are associated with familial amyotrophic lateral sclerosis. *Nature.* 362:59–62.

Sambrook, J., E.F. Fritsh, and T. Maniatis. 1989. Molecular Cloning: A Laboratory Manual. 2nd edition. Cold Spring Harbor Laboratory Press, Cold Spring Harbor, New York.

Sekizawa, T., H. Openshaw, K. Ohbo, K. Sugamura, Y. Itoyama, and J.C. Niland. 1998. Cerebrospinal fluid interleukin 6 in amyotrophic lateral sclerosis: immunological parameter and comparison with inflammatory and noninflammatory central nervous system diseases. *J. Neurol. Sci.* 154:194–199.

Shibata, N., A. Hirano, M. Kobayashi, T. Siddique, H.X. Deng, W.Y. Hung, T. Kato, and K. Asayama. 1996. Intense superoxide dismutase-1 immunoreactivity in intracytoplasmic hyaline inclusions of familial amyotrophic lateral sclerosis with posterior column involvement. *Neuropathol. Exp. Neurol.* 55: 481–490.

Sterneck, E., D.R. Kaplan, and P.F. Johnson. 1996. Interleukin-6 induces expression of peripherin and cooperates with Trk receptor signaling to promote neuronal differentiation in PC12 cells. *J. Neurochem.* 67:1365–1374.

Troy, C.M., N.A. Muma, L.A. Greene, D.L. Price, and M.L. Shelanski. 1990a. Regulation of peripherin and neurofilament expression in regenerating rat motor neurons. *Brain Res.* 529:232–238.

Troy, C.M., K. Brown, L.A. Greene, and M.L. Shelanski. 1990b. Ontogeny of the neuronal intermediate filament protein, peripherin, in the mouse embryo. *Neuroscience.* 30:217–237.

Tu, P.H., P. Raju, K.A. Robinson, M.E. Gurney, J.Q. Trojanowski, and V.M. Lee. 1996. Transgenic mice carrying a human mutant superoxide dismutase transgene develop neuronal cytoskeletal pathology resembling human amyotrophic lateral sclerosis lesions. *Proc. Natl. Acad. Sci. USA*. 93:3155–3160.

Tu, P.H., K.A. Robinson, F. de Snoo, J. Eyer, A. Peterson, V.M. Lee, and J.Q. Trojanowski. 1997. Selective degeneration of Purkinje cells with Lewy body-like inclusions in aged NFHLACZ transgenic mice. *J. Neurosci.* 17:1064–1074.

van Rijs, J., V. Giguere, J. Hurst, T. van Agthoven, A. Geurts van Kessel, S. Goyert, and F. Grosveld. 1985. Chromosomal localization of the human Thy-1 gene. *Proc. Natl. Acad. Sci. USA*. 82:5832–5835.

Williamson, T.L., L.I. Bruijn, Q. Zhu, K.L. Anderson, S.D. Anderson, J.P. Julien, and D.W. Cleveland. 1998. Absence of neurofilaments reduces the selective vulnerability of motor neurons and slows disease caused by a familial amyotrophic lateral sclerosis-linked superoxide dismutase 1 mutant. *Proc. Natl. Acad. Sci. USA*. 95:9631–9636.

Williamson, T.L., and D.W. Cleveland. 1999. Slowing of axonal transport is a very early event in the toxicity of ALS-linked SOD1 mutants to motor neu-

rons. *Nat. Neurosci.* 2:50–56.

Wong, P.C., C.A. Pardo, D.R. Borchelt, M.K. Lee, N.G. Copeland, N.A. Jenkins, S.S. Sisodia, D.W. Cleveland, and D.L. Price. 1995. An adverse property of a familial ALS-linked SOD1 mutation causes motor neuron disease characterized by vacuolar degeneration of mitochondria. *Neuron.* 14:1105–1116.

Xu, Z., L.C. Cork, J.W. Griffin, and D.W. Cleveland. 1993. Increased expression of neurofilament subunit NF-L produces morphological alterations that resemble the pathology of human motor neuron disease. *Cell.* 73:23–33.

Zhang, B., P.H. Tu, F. Abtahian, J.Q. Trojanowski, and V.M.Y. Lee. 1997. Neurofilaments and orthograde transport are reduced in ventral root axons of transgenic mice that express human SOD1 with a G93A mutation. *J. Cell Biol.* 139:1307–1315.

Zhu, Q., S. Couillard-Després, and J.P. Julien. 1997. Delayed maturation of regenerating myelinated axons in mice lacking neurofilaments. *Exp. Neurol.* 148:299–316.